Lifetime and dephasing of plasmons in Ag-nanoparticles

Mathias Scharte, Ron Porath, Torsten Ohms and Martin Aeschlimann[(a)]

Bernhard Lamprecht, Harald Ditlbacher and Franz R. Aussenegg[(b)]

[(a)] Department of Physics, University of Kaiserslautern, 67663 Kaiserslautern, Germany
[(b)] Institute for Experimental Physics, Karl-Franzens-University, Graz, Austria

ABSTRACT

In this work the dynamics of laser excited electrons in elliptic shaped silver nanoparticles were studied by means of the time-resolved two-photon-photoemission technique. The shape of the nanoparticles allows to distinguish between particle plasmon excitation and electron-hole pair excitation (intraband process) by simply changing the polarization of the laser pulse. These comparative studies, using the same experimental apparatus, enable us to study the respective role of collective and quasi-particle excitation in the electron dynamics of a metallic nanoparticle. The results are analyzed with a three level model according to the Liouville-von Neumann equation. The first measurements indicate that the electron dynamics vary considerably between these two excitation cases.

Keywords: plasmon, metallic nanoparticles, inhomogeneous linewidth broadening, photoelectron spectroscopy, energy dissipation

1. INTRODUCTION

It is a fundamental question, how physical properties change with the transition from a bulk metal piece to a metal particle with size well below the wavelength of light. The use of optical techniques to investigate nanoparticles is one of the most promising methods to advance our knowledge in this domain. Up to now extensive experimental as well as theoretical research has been done on the interaction of light with metal nanoparticles. For an overview, see [1-3].

In metal nanoparticles, collective electronic oscillations - the so called particle plasmons - can be excited by light and are therefore detectable as a pronounced optical resonance in the visible or UV parts of the spectrum. In recent years several linewidth measurements and time resolved SHG autocorrelation measurements on metallic nanoparticles have been published, reporting a dephasing time T_2 (also often called decay or damping time) of the localized particle plasmon excitation in the order of 6 fs to 10 fs [4-6].

Much less is known, however, about the microscopic mechanism of the investigated dephasing time T_2. Depending on certain conditions (such as size and size distribution, shape, dielectric constant of the surrounding medium etc.) the following possible mechanisms are proposed: First, the plasmon can decay by pure dephasing, e.g. a decay of the fixed phase correlation between the individual electronic excitation of the whole oscillator ensemble, described by T_2*. Possible mechanisms are scattering on surfaces or simple decay of the collective mode due to inhomogeneous phase velocities caused by the spread of the excitation energy or local inhomogeneity of the nanoparticles. Second, the plasmon can decay due to a transfer of the energy into a quasi-particle (electron-hole pair) or reemission of photons (luminescence), both described by T_1 [7].

The total dephasing of the plasmon is given by: $$\frac{1}{T_2} = \frac{1}{2T_1} + \frac{1}{T_2^*}. \quad (1)$$

In order to obtain a better understanding of the decay mechanism of the localized particle plasmon a deeper insight of collective oscillation as a many-body quantum system is necessary.

The present work focuses on the study of elliptic shaped metal nanoparticles with dimensions of 60 nm times 100 nm. The two-dimensional array of nearly identical, parallel oriented silver particles are deposited lithographically on a transparent ITO substrate which itself lays on a glass plate. Silver nanoparticles are of special interest as they can exhibit particularly strong size dependent optical extinction in the visible spectral range (1.8eV – 3eV) due to resonantly driven electron plasma oscillations.

Elliptic shaped metal nanoparticles show two different plasmon resonances which lie at different wavelengths for light polarized parallel to the short and long axes, respectively. Choosing the laser wavelength to one of these two resonances allows us to distinguish between plasmon excitation and electron-hole pair excitation (intraband process) by simply changing the polarization of the laser pulse. These comparative studies, using the same experimental apparatus, enable us to study the respective role of collective and quasi-particle excitation in the electron dynamics of a metallic nanoparticle. The measurements were performed in the low perturbation regime in order to avoid space charge effects and deformation of the metallic nanoparticles.

2. TIME-RESOLVED TWO-PHOTON-PHOTOEMISSION (TR-2PPE)

The experimental method used to investigate the lifetime of electronic excitations of the metal conduction band is time resolved two photon photoemission (TR-2PPE). This pump-probe technique enables a direct measurement of the

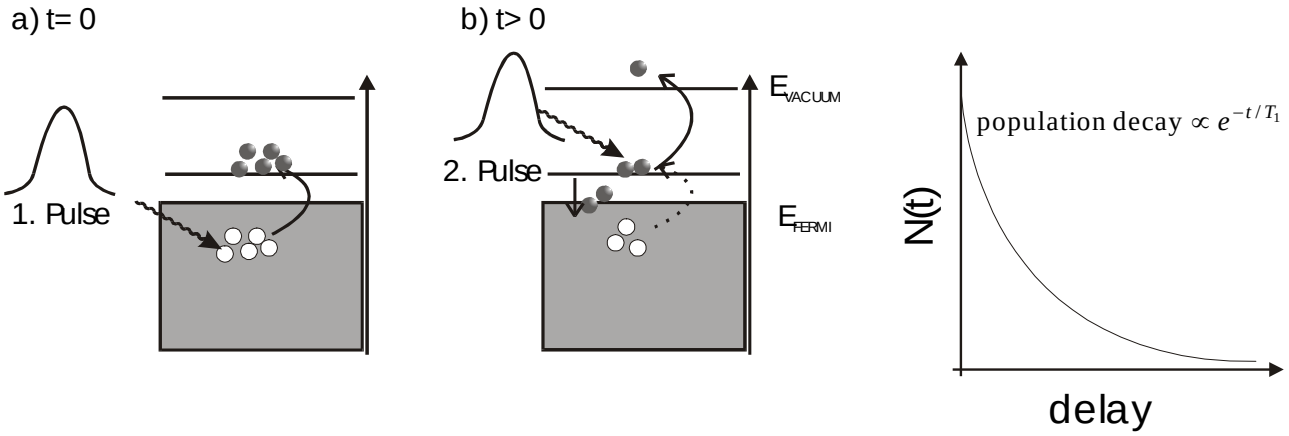

Figure 1: Principle mechanism of the time-resolved two-photon-photoemission (TR-2PPE) and the temporal behavior of the population N(t) in the intermediate state

dynamical properties in the time domain with a resolution of a few femtoseconds [8]. The principle is schematically shown in Figure 1. A pump pulse excites electrons out of the valence band into normally unoccupied states with energies between the Fermi and vacuum level. A second probe pulse measures the transient population of these intermediate states as a function of the temporal delay with respect to the pump pulse. The measured pump-probe-signal contains an exponentially decaying contribution which is, within a first order approach, directly correlated to the population decay time T_1 of the intermediate excitation state.

The experiments were performed with a femtosecond Kerr lens mode-locked Ti:sapphire laser (Tsunami, SpectraPhysics), pumped by about 10 W from a cw-operated diode pumped solid state (DPSS) laser (Nd:YVO_4, Millennia X, SpectraPhysics). The system delivers transform-limited and $sech^2$ temporal shaped pulses with up to 12 nJ/pulse and a duration of 40 fs at a repetition rate of 82 MHz and a wavelength of 830 nm. The linearly polarized output of the Ti:sapphire laser has been frequency-doubled in a 0.2 mm thick beta-barium-borate (BBO) crystal in order

to produce UV pulses at hν = 2.99 eV corresponding 415 nm. The UV beam was sent through a pair of fused silica prisms to pre-compensate for pulse broadening due to dispersive elements in the optical path to the sample like lenses, beamsplitters and the entrance window of the ultra-high vacuum chamber. In a Mach-Zehnder-interferometer the pulses are divided by a beamsplitter into equal intensity (pump and probe) pulses. Hereby one path is delayed with respect to the other by a computer-controlled delay stage. Both beams were combined collinearly by a second beamsplitter, sent through an adjustable λ/2-retardation plate and focused by means of a fused silica lens (f = 200 mm) perpendicularly to the sample surface. The diameter of the laser spot on the sample is around 100 µm. By means of the half wave plate it is feasible to rotate the plane of polarization to any arbitrary angle. This device resembles the so-called Savart plate. Nevertheless the light is always s-polarized on the surface of the sample.

The sample was held in an ultra-high vacuum chamber at a base pressure in the 10^{-10} mbar range. A bias of – 4 V was applied to the sample to eliminate the effects of any stray electric fields. The photoemitted electrons were detected in a cylindrical spherical analyzer (CSA). The entrance axis of the energy analyzer is 45° with respect to the laser beam. In general, we used a pass energy of 4 eV, leading to roughly 50 meV resolution.

3. ELLIPTIC-SHAPED SILVER NANOPARTICLES ON ITO

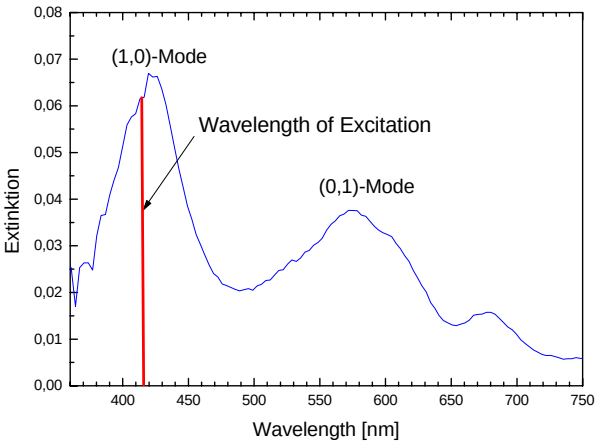

Figure 3: Extinction spectrum of a nanoparticle array

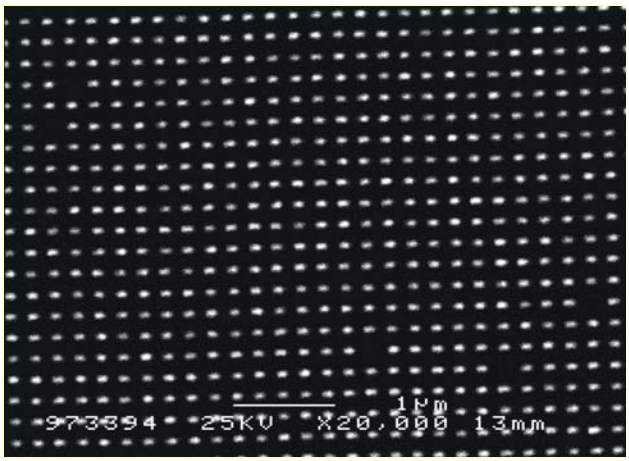

Figure 4: SEM picture of lithographically fabricated nanoparticles on ITO

The elliptic-shaped silver nanoparticles have a size of 60 nm times 100 nm and have a thickness of 60 nm. Figure 2 illustrates the shape and the resonance orientations. The short half axis of the elliptic particle is denoted ‘h’. Incoming light that is polarized parallel to this axis excites resonant plasmon oscillations. The nanoparticle has two different resonance frequencies as visible in the extinction spectrum (Figure 3). The whole quadratic array containing the particles has an extent of 240 µm lateral length. The substrate is a 30 nm thick layer of indium-tin-oxide (ITO) which itself is applied on an ordinary quartz glass plate. ITO was used because on one hand it is electrically conducting to prevent charging effects but on the other hand the amount of photoemitted electrons coming from its surface are negligible. For a controlled design of the metallic nanoparticles an electron beam lithography technique was used [9,10]. In Figure 4 a SEM picture of a sector of such an array is shown. As particle shape and interparticle distance can be varied independently, this method allows to tailor the optical properties of the single particles. Thus resonance frequency and the strength of particle interaction can be tuned independently. Thereby the optical extinction maximum can be tuned to the desired wavelength (in this case to the illuminating laser wavelength of 415 nm). For the electron beam lithographic process the substrate was spin coated with a 60 nm thick polymethylmethacrylate (PMMA) layer, which serves as a positive e-beam resist. Then exposure is performed by using an e-beam writing

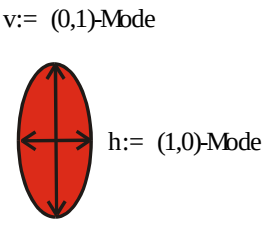

Figure 2: Resonance orientations within the elliptic shaped nano-particle

equipment consisting of a scanning electron microscope and a pattern generator, i.e. a computer with the appropriate hardware and software. After the development process the samples are coated by a 60 nm thick silver layer by e-beam evaporation. In the following lift-off process the metal coated PMMA layer was removed, whereas the e-beam exposed areas are now coated with silver, which remains on the ITO.

4. THEORETICAL ANALYSIS OF TIME-RESOLVED TWO-PHOTON PHOTOEMISSION

For interpretation of the observed time response we used a density matrix formalism which accounts for energy and phase relaxation for a three level system on a phenomenological basis (Figure 5). For the propagation of the density

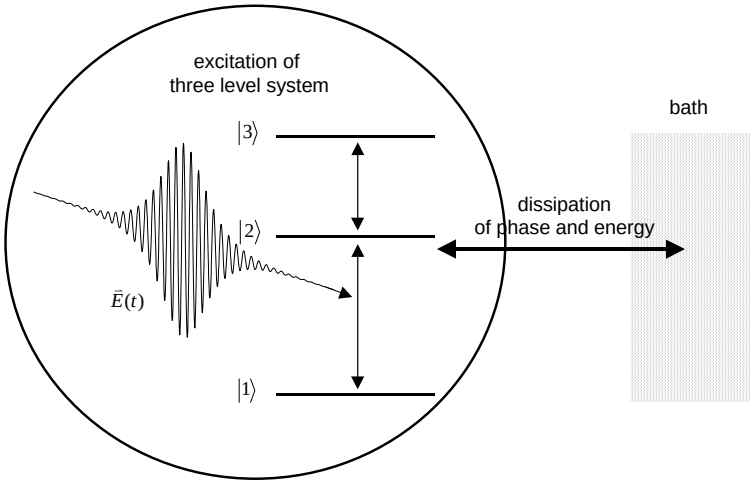

Figure 5: System considered within the used density matrix formalism. The disturbing Hamiltonian operator is given by the interaction of a three-level system with an electromagnetic field. The dissipative terms are determined by the coupling to an external bath.

matrix we use the Liouville-von Neumann equation. This equation follows the common formalism of a density matrix and can be seen as a quantum mechanical attempt to describe the interaction of an electronic system with an electromagnetic field [11]:

$$\frac{d}{dt}\rho = -\frac{i}{h}[H,\rho] + \frac{d}{dt}\rho^{diss.} \tag{2}$$

Here the density matrix ρ is defined by its elements $(\rho)_{nm} = |n\rangle\langle m|$ where n and m denote the different energy levels. The diagonal elements $(\rho)_{nn}$ give the probability of the system being in the state $|n\rangle$, while $(\rho)_{nm} = (\rho)^*_{mn}$ represent the optically induced coherence between $|n\rangle$ and $|m\rangle$. The dissipative term $\frac{d}{dt}\rho^{diss.}$ describes the temporal decay of the respective elements of the density matrix due to coupling to an external bath. The interaction with this reservoir gives rise to energy and phase loss processes.

The potential of the Liouville–von Neumann formalism for describing the three-step excitation mechanism of TR-2PPE was shown by Hertel *et al.* [12], who achieved a consistent description of the spectroscopy (2PPE) *and* dynamics (TR-2PPE) of the (n=1) image-potential states on a Cu(111) surface. Also Bauer *et al.* [13] demonstrated successfully the capability of that formalism in their investigations of photoexcited alkali chemisorbates. In addition, Ogawa *et al.* [14] succeeded in simulating the non-resonant excitation of an image-potential state, as obtained by means of interferometric TR-2PPE. This model is, in principle, exact valid for describing a system of three discrete states only.

It has to be noted that the Liouville-von Neumann formalism is a simplified representation of the real excitation process between bands in a metal.

In case of a pure three-level system one obtains a set of nine coupled differential equations. Five free parameters are left i.e. the decay of the population of state $|2\rangle$ and $|3\rangle$ and the dephasing of all three states [13]. The number of free parameters is further reduced by the following assumptions:

1.) Dephasing of state $|3\rangle$ is set to zero [13]

2.) Dephasing of state $|1\rangle$ is chosen as 2 fs [15]

3.) Decay of state $|3\rangle$ is set to zero [13]

What finally remains is the population decay of state $|2\rangle$ which is quantified by T_1 and the pure dephasing of the same state which is quantified by T_2^*. Both values lead to the formula for the total dephasing as introduced in equation (1).

5. RESULTS AND DISCUSSION

Figure 6 shows the photoemission yield as a function of the polarization angle of the laser pulse. Clearly visible is the strong rise of the 2PPE-signal in the case of plasmon excitation (denoted by 'h', see Figure 2) compared to electron-hole pair excitation (denoted by 'v'). The shape of the 2PPE photoemission spectra, however, do not show distinct differences by an excitation in the 'v' or 'h' direction. The resonant enhancement of the photoemission yield can be explained by the enlarged absorption of light by an extinction in the (1,0)-mode and by the lightning rod effect [16] meaning that the field enhancement can occur simply due to a concentration of the electric field at positions of maximum curvature (tip effect).

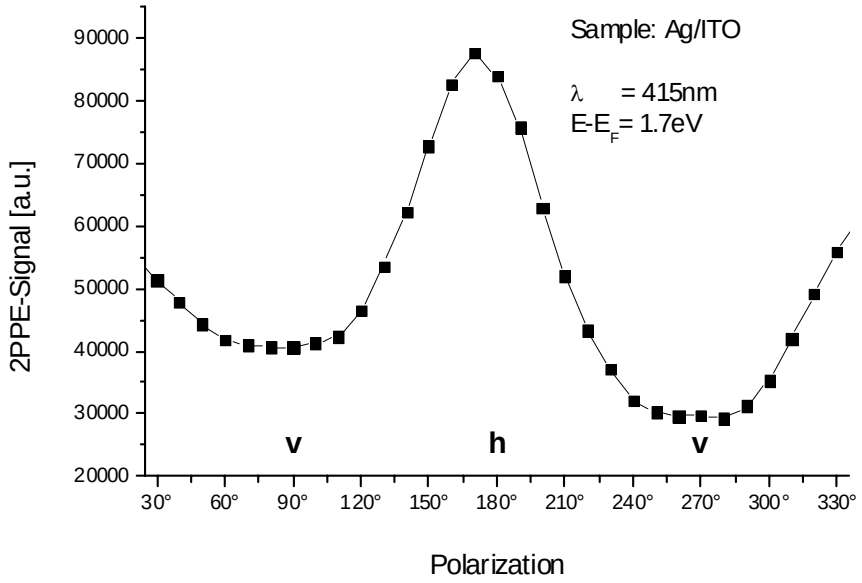

Figure 6: 2PPE yield versus polarization. In case of the plasmon excitation ('h') a strong rise in the 2PPE-signal occurs.

Figure 7 shows the FWHM determined from the autocorrelation traces of the TR-2PPE measurement as a function of the rotation of the state of polarization. Each data point is represented by the FWHM of a $sech^2$-shaped curve that is fitted into the autocorrelation measurement. A typical autocorrelation measurement is shown in the inset. For comparison also the behavior of polycrystalline tantalum is shown. The FWHM for tantalum is not affected by turning the polarization angle of the incoming light. Therefore, any effect caused by an increasing of the dispersion due to rotation of the half wave plate can be excluded. As one can see the FWHM reduces by rotation of 90° from almost 75 fs in the 'h' direction (plasmon excitation) to 69 fs in the 'v' direction (electron-hole pair excitation). Further rotation restores the long lifetime of the plasmon excitation case. One should note that these FWHM

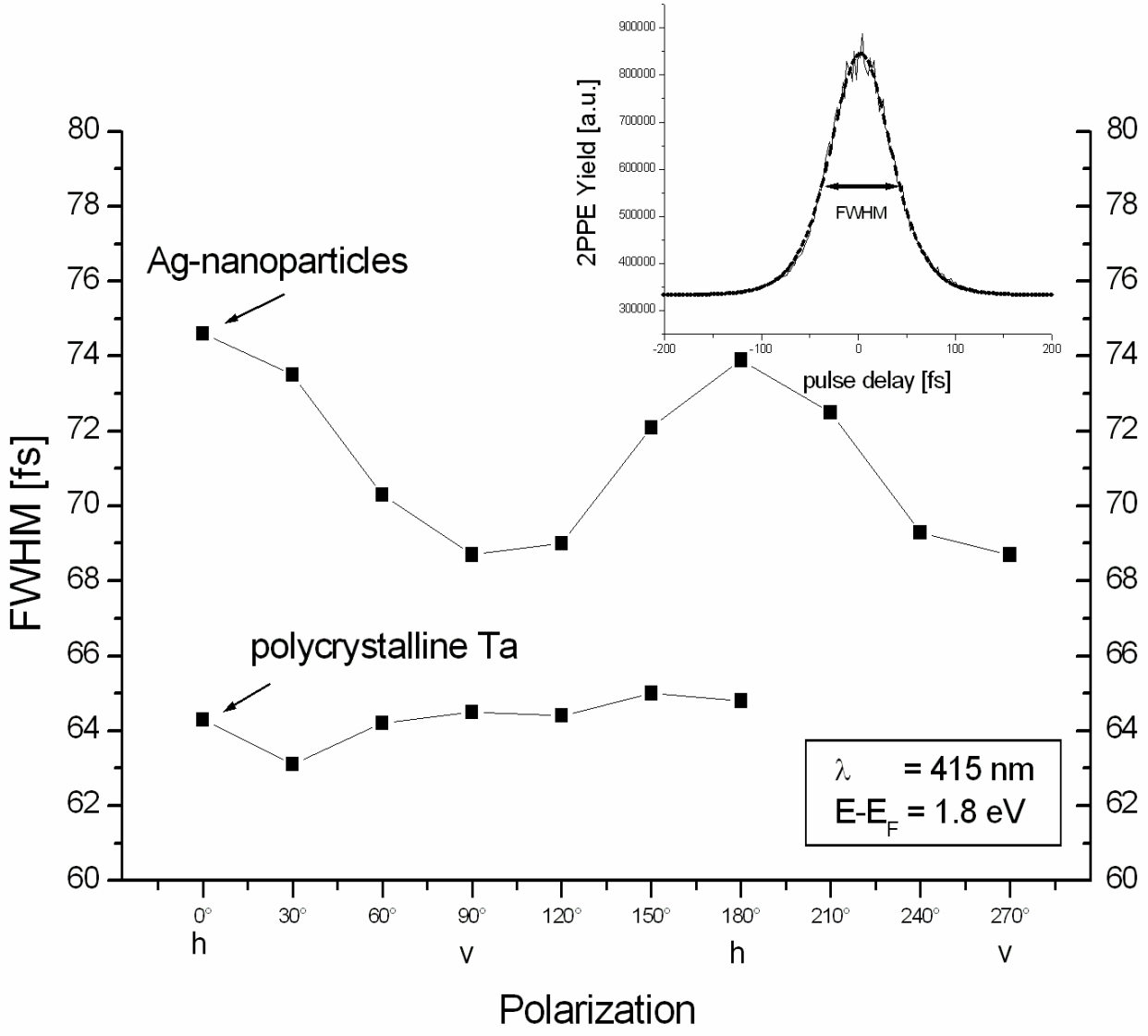

Figure 7: Nanoparticles show a variation of the FWHM of the autocorrelation over rotating states of polarization while tantalum shows no effect. In the inset a typical autocorrelation measurement can be seen from which the data points have been derived.

values still include the autocorrelation of the laser pulse width. But obviously, collective and quasi-particle excitation result in a rather different electronic relaxation behavior.

In order to obtain a deeper insight of the electron dynamics in the fs time scale, the results are analyzed by the Liouville-von Neumann equation as discussed above. According to equation (1), two free parameters are left: the inelastic lifetime T_1 and the pure dephasing time T_2^* of the intermediate state $|2\rangle$. In the following, one of these two free parameters is held invariable at a chosen value according to the different suggested damping mechanism of a collective excitation. All corresponding values are presented in Table 1:

a.) The model of pure dephasing

This model is based on the assumption that the difference in TR-2PPE data of Figure 7 between collective and quasi-particle excitation is merely caused by an increase in the pure dephasing time in the collective excitation case. The energetic decay as described by T_1 remains in both cases the same. In the quasi-particle excitation mode ('v') we

assume the ordinary rapid dephasing [15] and specify T_2^* to 2fs. As a consequence our fitting simulation delivers 11 fs for T_1. Taking into account that this model is based on an identical energetic decay time T_1 for both excitation cases we obtain a pure dephasing time T_2^* of approximately 95 fs for the plasmon excitation mode ('h'). Noteworthy is that in this model the total dephasing time T_2 becomes rather large (around 17 fs) compared to the value of 6 fs as obtained by pure optical methods.

b.) The model of change in inelastic lifetime

In this second model solely the energetic decay is responsible for the various electron dynamics. Therefore, T_2^* is chosen to be 2fs in both cases (rapid dephasing). The inelastic lifetime T_1 is influenced by scattering processes with cold electrons (electron-hole decay), which can be damped in a collective excitation. The fitting results in T_1 = 11 fs for the quasi-particle excitation mode ('v') and 17 fs for the plasmon mode ('h'). In this model the total dephasing time T_2 becomes rather small (around 2 fs).

c.) The model of fitting pure optical results

In this model we try to fit our data with linewidth measurements of pure optical methods, assuming a decay of the plasmon by pure dephasing of the collective mode. Therefore, we set T_2^* to be 6 fs as specified by Lamprecht *et al.* [4]. The fitting for the plasmon mode results in a inelastic lifetime T_1 = 15 fs.

$E-E_F$ = 1.8 eV	T_1 [fs]	T_2 [fs]	T_2^* [fs]	model
h (plasmon) v (electron-hole-pair)	11 **11**	$(1/22 + 1/95)^{-1}$ $(1/22 + ½)^{-1}$	**≈95** 2	change of pure dephasing
h (plasmon) v (electron-hole-pair)	**17** **11**	$(1/34 + ½)^{-1}$ $(1/22 + ½)^{-1}$	2 2	change of inelastic lifetime
h (plasmon) v (electron-hole-pair)	**15** **11**	$(1/30 + 1/6)^{-1}$ $(1/22 + ½)^{-1}$	6 2	change of inelastic lifetime assuming T_2^* to be 6 fs

Table 1: Fitting parameters for different models. Non-bold values were fixed and bold values are results of the fitting routine

6. CONCLUSION

In this paper we reported on femtosecond time-resolved two-photon photoelectron studies of elliptic shaped silver nanoparticles. By simply changing the polarization of the laser pulse, we were able to distinguish between plasmon excitation (horizontal polarization) and electron-hole excitation (Drude absorption, vertical polarization). We found a clear difference in the observed autocorrelation traces by these comparative studies. The results are analyzed with a three level model according to the Liouville-von Neumann equation. Assuming an equal inelastic lifetime T_1 for plasmon and electron-hole excitation of 11 fs, we obtained a pure dephasing time T_2^* of about 95 fs for an optically excited plasmon. However, on the other hand a model based just on a change in the energetic decay (T_1) would result in a pure dephasing time of 2 fs. Also a mixture of these two models might be possible, leading to a change in T_1 and T_2.

ACKNOWLEDGEMENTS

We would like to thank W. Pfeiffer and A. Liebsch for valuable discussions. This work was supported by the Deutsche Forschungsgemeinschaft (DFG) and the Austrian Ministry for Technology, the Austrian Science Foundation, grant No. P14292 and the European Union, TMR project NanoSNOM.

REFERENCES

1 C. Bohren and D. Huffmann, *Absorption and scattering of light by small particle*, John-Wiley, New York, 1983.

2 U. Kreibig and M. Vollmer, *Optical properties of metal clusters*, Springer, Berlin, 1995.

3 J.-Y. Bigot, V. Halté, J.-C. Merle, A. Daunois, *Chem. Phys.*, **251**, p. 181 (2000)

4 B. Lamprecht, A. Leitner and F.R. Aussenegg, *Appl. Phys. B*, **68**, 419 (1999)

5 T. Vartanyan, M. Simon and F. Träger, *Appl. Phys. B*, **68**, 425 (1999)

6 T. Klar, M. Perner, S. Grosse, G. von Plessen, W. Spirkl and J. Feldmann, *Phys. Rev. Lett*, **80**, 4249 (1998)

7 J. Lehmann, M. Merschdorf, W. Pfeiffer, A. Thon, S. Voll and G. Gerber, *Phy. Rev. Lett.*, **85**, p. 2921 (2000)

8 C.A . Schmuttenmaer, M. Aeschlimann, H.E. Elsayed-Ali, R.J.D. Miller, D. Mantell, J. Cao and Y. Gao; *Phys. Rev. B.* **50**, p. 8957 (1994)

9 W. Gotschy, K. Vonmetz, A. Leitner and F. R. Aussenegg, *Appl. Phys. B* **63** 381 (1996).

10 W. Gotschy, K. Vonmetz, A. Leitner and F. R. Aussenegg, *Opt. Lett.* **21** 1099 (1996).

11 R. Loudon, *The Quantum Theory of Light*, Oxford University Press, Oxford, 1973

12 T. Hertel, E. Knoesel, A. Hotzel, M. Wolf and G. Ertl, *J. Vac. Sci. Technol.*, A **15(3)**, p. 1503 (1997)

13 M. Bauer, S. Pawlik and M. Aeschlimann, *Phys. Rev. B* **60**, p. 5016 (1999)

14 S. Ogawa, H. Nagano, H. Petek and A.P. Heberle, *Phys. Rev. Lett.* **78**, p. 1339 (1997)

15 H. Petek and S. Ogawa, *Prog. Surf. Sci* **56**, 239 (1997)

16 A. Wokaun, in *Solid State Physics*, p. 223, H. Ehrenreich, T. Thurnbull and F. Seitz, Eds., Academic, New York 1984.